

Polymer Testing

April 2015, Volume 171, Pages 87-95

<http://dx.doi.org/10.1016/j.polymeresting.2015.02.004><http://archimer.ifremer.fr/doc/00252/36371/>

© 2015 Elsevier Ltd. All rights reserved.

Archimer<http://archimer.ifremer.fr>

Moisture sorption in polyamide 6.6: experimental investigation and comparison to four physical-based models

Broudin M.^{1,3}, Le Saux V.^{1,*}, Le Gac Pierre-Yves², Champy C.³, Robert G.⁴, Charrier P.³, Marco Y.¹

¹ Laboratoire Brestois de Mécanique et des Systèmes (EA 4325), ENSTA Bretagne/Université de Brest/ENIB, 2 rue F. Verny, 29806 Brest Cedex 9, France

² Materials and Structures Group, IFREMER (French Ocean Research Institute), Centre de Brest, BP 70, 29280 Plouzané, France

³ TrelleborgVibracoustic, Z.I. Nantes Carquefou, BP 419, 44474 Carquefou Cedex, France

⁴ Solvay Engineering Plastics, Technyl Innovation Center-Simulation et Validation des Applications, Avenue Ramboz – BP64 – 69192 Saint Fons, France

* Corresponding author : V. Le Saux, tel.: +33 (0)2 98 34 87 18 ;

email address : vincent.le_saux@ensta-bretagne.fr

Abstract :

Water sorption in polyamide 6.6 has been characterized for a wide range of temperature (25°C to 80°C) and various water activities using a Dynamic Vapor Sorption testing machine. Complex sorption mechanisms govern the water uptake in the material. The competition between two main temperature dependant mechanisms has been observed: a Henry's sorption mechanism that mainly governs the sorption curve at low water activities, and a second mechanism at high water activities that could be related to the formation of water clusters. It is observed that the temperature dependency can mainly be attributed to the Henry's contribution. Four physically based models are then used and identified thanks to the extended experimental database. It is shown that a simple Flory-Huggins model is not able to capture the experimental observations at very high water activities for all the temperatures tested. The ENSIC model is a better choice, but good prediction for very high water activity cannot be obtained. Both modified Park and GAB models can accurately predict the volume fraction of water for the whole ranges of water activity and temperature, although the modified Park model should be preferred considering the number of parameters and the mathematical simplicity.

Keywords : polyamide 6.6, water sorption, temperature, relative humidity, physically-based models

1. Introduction

In order to reduce CO₂ emission and fuel consumption, the automotive industry wishes to reduce the mass of vehicles. Short glass fiber reinforced polyamide 6.6 composites are appropriate candidates because they combine an affordable price and a reasonable stiffness thanks to the complex shapes allowed by the injection molding process. These materials are not new in the automotive industry, they have been used for a long time for parts submitted to limited thermo-mechanical loading. They are nowadays increasingly used for structural applications such as engine mounts or clutch pedals (Figure 1) that are submitted to complex cyclic movements. Furthermore, important variations of the temperature and relative humidity can be induced by the service conditions (under-bonnet temperature and climatic variations) [1]. Both temperature and relative humidity are known to have a strong impact on the mechanical properties of polyamide [2-5].

Fig. 1 – TrelleborgVibracoustic engine mount with PA6.6 50%wtGF housing for PSA.

The strong influence of the relative humidity on the mechanical response is especially high for polyamide because of the hydrophilic nature of the amide functional group [6]. In the case of unfilled polyamide 6.6, saturation values of water absorption up to 8.5% at 23°C and relative humidity of 100% are commonly found in the literature [7]. The absorption of water in the polyamide leads to at least three consequences. The first is modification of the matrix behavior: the ultimate strain increases and the material stiffness decreases [2, 5]. The second is the reduction of the glass temperature transition T_g with the increase of water content. A reduction of nearly 60°C when the relative humidity ratio is increased from 0 to 80% (T_g varies from 320K to 260K) is, for example, reported [7]. The last consequence is swelling of the structure that induces dimensional changes that can be problematic for the integration of the structure in its environment [8]. Moreover, in many industrial parts submitted to demanding loading, the concentration of water in the material is not homogeneous. Thus, understanding of the water gradient and the consequences on the mechanical and physical properties variations with time, but also with position, is mandatory to predict the thermo-mechanical response needed to get a reliable design.

The classical way to investigate the water sorption consists of monitoring the global mass uptake using gravimetric analysis. Two main quantities can be defined from these

experiments: the equilibrium mass uptake (*i.e.* the maximum water content absorbed by the polymer) and the time needed to reach this saturation state characterized by the diffusion coefficient. In this paper, we choose to focus only on the equilibrium mass uptake; the analysis of the diffusion coefficient will be discussed in a forthcoming paper. Dealing with equilibrium water content, the early studies performed by Barrie in 1968 [9], highlighted the diversity of sorption mechanisms. The amount of sorbed water at equilibrium increased almost linearly over a wide range of water activities obeying Henry's law isotherm, except for at low and high relative humidity. The deviation at low relative humidity classically appears as a "shoulder" and is typical of type "II" isotherms [10] classically modeled with a Langmuir type sorption. At high water activities, the equilibrium water uptake rises sharply, which could be related to water clustering [11]. For water absorption in PA6.6, several studies have already noted that the Langmuir type sorption is absent [6, 12, 13], and the water sorption isotherm is composed of only two zones: that following Henry's law at low activities and Flory-Huggins type sorption.

Indeed, the experimental databases found in the literature are usually restricted to a limited range of temperatures and water activities, not consistent with the ranges seen by industrial structures, especially automotive structures. Therefore, the first aim of this paper is to build an experimental database as thorough as possible covering a wide range of temperature and humidity ratio. The literature provides a wide range of models, so the other aim of the paper is to challenge the experimental database and compare the predictability of four physically-based models classically found in the literature (Flory Huggins [14, 15], ENSIC [16], Park [17] and GAB [18-20]). The restriction to physically based models is motivated by the idea that the extrapolation to a wider range of temperature of such models is more reasonable as long as the underlying hypotheses of this model are known, which is usually not the case for empirical models.

The paper is divided into 5 sections. First, the material and experimental used to build the database are briefly detailed. It should be pointed out that we chose to focus in this paper on polyamide 6.6 matrix only. The investigation of the influence of fibers on the ability of the material to absorb water is considered as a perspective of this work. Moreover, in order to limit as much as possible the time needed to build an extended database, the measurements were performed on thin films, rather than on thick plates, as classically done in the literature. The experimental results are then presented and the key points are highlighted. Various

models are then presented and their ability to capture the specificities of the experimental database is then discussed. Finally, conclusions are proposed.

2. Materials and methods

2.1 Materials and samples

The material used is a polyamide 6.6 matrix provided by Solvay® (A218nat) with a density of 1.14 g/cm^3 , and a molecular weight of $16\,500 \text{ g/mol}$. The glass transition temperature of the polymer in the dry state has been evaluated at $56 \pm 1^\circ\text{C}$ with classical DMTA tests using the three tangents method on the storage modulus E' . Thin films of $100 \mu\text{m}$ thickness were cut from injected plates using a Leica microtome.

2.2 Gravimetric experiments and construction of the sorption curves

The gravimetric experiments were performed using a Dynamic Vapor Sorption (DVS) Q5000SA, TA Instruments, equipped with a high-accuracy micro-balance ($0.1 \mu\text{g} \pm 1\%$). The accuracy of the system is $\pm 1\%$ for the RH over a range of 0-98% and $\pm 0.1^\circ\text{C}$ for the temperature stability. During a DVS measurement, the sample can be subjected to varying humidity and temperature conditions, and the mass of the sample is measured continuously during the test. To simplify the interpretation of our measurements, the temperature remained fixed whereas the humidity ratio was changed in order to build isothermal water sorption curves.

Before being exposed to any vapor, the samples were dried at 0% RH to remove any surface adsorbed vapor and to establish a dry mass baseline. The samples were then exposed to carrier air with varying relative humidity obtained by mixing flows of dry and wet nitrogen at 200 ml/min . The relative humidity was increased step by step during adsorption. The time of each step was chosen such that the weight equilibrium was reached. The next step then starts from this new equilibrium state. Figure 2 presents an illustration of a typical result where water activity is progressively increased from a value of 0 to 0.85. It should be pointed out that the maximum water activity reached during the DVS measurement is temperature dependant and chosen so that no condensation occurs in the test apparatus (values are chosen as given in the documentation of the test apparatus).

Fig. 2 – Example of DVS result obtained for a temperature of 40°C. The mass evolution $\Delta m = m_t - m_0$ is plotted versus time

Because RH of 100% cannot be obtained using the DVS measurements, two complementary points were also obtained by classical gravimetric analysis at 25°C and 80°C by immersing the samples in water. The main purpose of these points is to have data in a specific range where a small increase of relative humidity can have an important impact on the maximum sorbed water, and can thus challenge the model identification and predictability. As these tests are performed on plates and not thin films, several complementary points were also defined to make sure that the experimental results that come from DVS and classical gravimetric analysis are comparable. Figure 3 plots the data obtained using DVS measurements and classical gravimetric analysis, and more specifically the value at saturation for a temperature of 25°C (the meaning of the quantity v_{H_2O} will be explained in the next paragraph). No specific differences are noticed between the two techniques. We can, therefore, use both techniques to build our experimental database. Common points are omitted to simplify the database and only those from DVS are kept (except for RH of 100%).

Fig. 3 – Comparison between DVS measurements and classical gravimetric analysis for a temperature of 25°C.

Sorption isotherms are obtained by plotting the mass evolution at sorption equilibrium versus the water activity defined as:

$$a = \frac{p}{p_{sat}} \quad (1)$$

where p is the vapour pressure of water in the environment and p_{sat} the saturated pressure of water at the same temperature. The mass evolution is calculated according to:

$$\Delta m = m_t - m_0 \quad (2)$$

where m_t is the mass of the sample at time t and m_0 is the mass of the sample in the dry state. It is usually convenient to define the evolution of the mass absorption ratio M_t :

$$M_t = \frac{m_t - m_0}{m_0} \quad (3)$$

As polyamide 6.6 is a semi-crystalline polymer and as water diffuses only in the amorphous phase [2], the sorption mechanism will be considered only over the combination of water and

amorphous phase. The relative mass ratio w_{H_2O} and relative volume ratio v_{H_2O} will be considered here and can be defined as:

$$w_{H_2O} = \frac{\Delta m}{(1-\chi)m_0 + \Delta m} = \frac{M_t}{M_t + (1-\chi)} \quad (4)$$

$$v_{H_2O} = \frac{w_{H_2O}\rho_a}{w_{H_2O}\rho_a + (1-w_{H_2O})\rho_w} \quad (5)$$

where ρ_a and ρ_w are the respective densities of the amorphous phase of the polymer and water. Their values will be taken equal to 1080g/cm^3 for ρ_a [21] and 1000g/cm^3 for ρ_w .

3. Experimental results

We present in this section the experimental results and highlight some specifics of the studied material. Figure 4 plots the volumetric fraction of water in the amorphous phase of the versus the water activity for all the temperatures tested. Several aspects can be pointed out. Prior to any misleading interpretation, an experimental scattering analysis has to be performed in order to make sure that the results are related to a physical phenomenon and not to the experimental scatter. The results of 3 tests performed on 3 different samples for a temperature of 40°C degree and the mean values as well as the standard deviation are plotted in Figure 4. We can note that this standard deviation is lower than the differences induced by the temperature on the sorption curves. Therefore, the temperature dependency has to be taken into account since it is related to a physical phenomenon.

Then, we see in Figure 4, as expected, different behaviour in the isotherm sorption at lower and higher water activities [12, 13, 22]. It is observed that the isotherms display an upward curvature that becomes more and more pronounced as activity increases. No initial curvature at low activities is noticed, with no Langmuir sorption phase, which is a classical result for PA6,6 matrix [6, 12, 13]. The sorption curve can be described by a linear curve at low activities according to Henry's behaviour. At high activity ($a > 0.6$), a deviation from this linear part is seen that can be explained by to the formation of water clusters [6, 11].

Fig. 4 – Sorption curves for all the testing temperature.

The second point is that the sorption isotherms depend on the temperature. To highlight this phenomenon, Figure 5 plots the volume fraction of water in the amorphous phase of the PA66 matrix versus the temperature for various water activities. It can be clearly pointed out that the higher the temperature, the lower the v_{H_2O} value (for a given water activity). This result stands for all the water activities studied.

Fig. 5– Effect of the temperature on the sorption curves.

The dependency of the maximum water uptake on the temperature is a classical result for highly hydrophilic polymers, such as certain epoxide-amine networks [23], but is quite unusual for PA66 [13, 24] where the maximum water uptake was found to be almost temperature independent. This result encouraged consideration of this uptake as well representative of the water-polymer interaction [12]. However, this temperature dependant behavior has already been noted in the literature for PA66 [6], and can be physically explained by Henry's law [25]. Dealing with our experimental results, it seems that the main differences occur on the initial slope (related to the Henry behavior). The non linear contribution does not seem affected by the temperature, as the shape of the curves does not evolve with temperature for high water activities. To highlight this, Figure 6 plots the experimental results already presented in Figure 4 but where the linear contribution (that is temperature dependant) has been subtracted to isolate the non linear part of the curve strongly related to water clustering [11].

Fig. 6 – Effect of the temperature on the nonlinear contribution of the sorption curves obtained by subtracting the linear contribution evaluated experimental data for water activities up to 0.4.

To obtain these data, the initial slope of each curve was estimated for each temperature using the data obtained for water activities up to 0.4. We can clearly see independence of the non linear contribution to the temperature, leading to the conclusion that the dependency of the maximum water uptake to the temperature can be taken into account in the linear contribution, *i.e.* the Henry one.

4. Models and identification

We discuss in this section the model candidates to reproduce the experimental results and, more specifically, to focus on a way to integrate the effect of temperature on the sorption curves. We chose to consider 4 different models that are widely used in the literature. Before briefly presenting the models, we describe the numerical strategy we set up to identify the constitutive parameters of these models. This strategy is the same for all models.

4.1 Identification strategy

The constitutive parameters of the models are identified thanks to an optimization procedure based on a least squares fitting. The parameters are found such as they guarantee:

$$\min_p \sum_{i=1}^N [s_i(a_i^{\text{exp}}, T^{\text{exp}}, p) - y_i(a_i^{\text{exp}}, T^{\text{exp}})]^2 \quad (6)$$

where p represents the model parameters array, s is the response of the model for a given activity and temperature, y corresponds to the experimental data obtained for a given temperature and activity and N is the number of experimental observations. As several temperatures are considered, the global error array is obtained by concatenating the array obtained for each temperature. Therefore, the strategy used here is a global one, *i.e.* the identification is performed considering the whole database and for each temperature independently. The identification is performed using a python script that uses the function “leastsq” given in the optimization toolbox of the “scipy project” [26]. The function uses a gradient-based Levenberg-Marquardt algorithm. To start the algorithm, an initial point must be provided. For each model, these parameters are chosen consistent with its physical meaning. Sensitivity analysis of the results to this initial guess was systematically done afterwards in order to make sure that the final parameters do not depend on this initial guess and can, therefore, be considered as the optimum ones.

In order to be able to compare qualitatively the model identification, a scalar value, termed Determination Coefficient, is calculated according to:

$$DC = 1 - \frac{\sum_{i=1}^N (y_i(a_i^{\text{exp}}, T^{\text{exp}}) - s_i(a_i^{\text{exp}}, T^{\text{exp}}, p_{opt}))^2}{\sum_{i=1}^N (y_i(a_i^{\text{exp}}, T^{\text{exp}}) - \bar{y})^2} \quad (7)$$

where \bar{y} represents the mean value of the array y :

$$\bar{y} = \frac{1}{N} \sum_{i=1}^N y_i \quad (8)$$

and p_{opt} the “optimum” set of parameters. The DC quantity evolves between 0 and 1. A value of 0 means very poor correlation (the model should be avoided) and a value of 1 means excellent correlation.

4.2 Flory-Huggins model (1942)

Flory [14] and Huggins [15] developed in the 40s a mean-field theory used to describe sorption in polymers based on a statistical analysis of the different configuration of a polymer/solvent system using a lattice conception, which still remains the basis for new more refined theories. The model has the following simple form:

$$\ln(a) = \ln(v_{H_2O}) + (1 - v_{H_2O}) + \gamma(1 - v_{H_2O})^2 \quad (9)$$

where a is the water activity of the surrounding air, v_{H_2O} the volumic fraction of water absorbed in the matrix and γ is the Flory-Huggins interaction parameter that can be temperature dependant [12] according to a classical Arrhenius equation:

$$\gamma = \gamma_0 \exp\left(\frac{E_a^\gamma}{RT}\right) \quad (10)$$

This parameter is a reflection of the polymer/solvent affinity, where the lowest γ value describes the highest sorption level and, thus, the best affinity. Figure 7 presents the comparison between the models prediction with the optimum parameters and the numerical results for the 4 tested temperatures. The best parameters are given in Table 1.

Fig. 7 – Prediction of the volume fraction of water in the amorphous phase for the Flory-Huggins model at various temperatures.

Parameter	Value
γ_0	3.852
E_a^γ	2107 [kJ/mol]
DC@25°C	0.9852
DC@40°C	0.9926
DC@60°C	0.9869
DC@80°C	0.8999

Tab. 1 – Optimum parameters for the Flory Huggins model.

4.3 ENSIC model (1996)

The ENgaged Species Induced Clustering (ENSIC) model has been developed more recently [16]. This model considers the probability of insertion of a non-polymeric molecule in a system that contains only two types of species, *i.e.* the polymer and the sorbed molecules, the latter being present only in its condensed phase. Based on a basic lattice concept, the following relation was derived:

$$v_{H_2O} = \frac{k_p}{k_s - k_p} [\exp((k_s - k_p) \cdot a) - 1] \quad (11)$$

The key parameters are the elementary affinity between the non-polymeric species (water molecules here) and either a polymer site (k_p) or a previously sorbed solvent molecule (k_s). One particular characteristic of this model is its ability to describe Langmuir type sorption, Flory-Huggins-like isotherms or Henry sorption depending on the values of k_s and k_p . Moreover, this model enables solvent clustering as long as the solvent/solvent affinity (k_s) is higher than the solvent/polymer affinity (k_p). Based on the experimental observation and the physical meaning of the parameters, a possible extension in order to make the model temperature dependant would be to suggest evolution of the k_p with temperature according to:

$$k_p = k_{p0} \exp\left(-\frac{E_a^{k_p}}{RT}\right) \quad (12)$$

Figure 8 presents the comparison between the models prediction with the optimum parameters and the numerical results for the 4 tested temperatures. The best parameters are given in Table 2.

Fig. 8 – Prediction of the volume fraction of water in the amorphous phase for the ENSIC model at various temperatures.

Parameter	Value
k_{p0}	0.0251
$E_a^{k_p}$	-1889 [kJ/mol]
k_s	1.596

DC@25°C	0.9965
DC@40°C	0.9923
DC@60°C	0.9853
DC@80°C	0.9960

Tab. 2 – Optimum parameters for the ENSIC model.

4.4 Modified Park model (1986)

Based on the assumption that three different physical mechanisms can explain the shape of a sorption isotherm curve (Langmuir, Henry and clustering phenomena), Park [17] suggests a simple mathematical representation based on the decomposition of these phenomena:

$$v_{H_2O} = \frac{Ab_L a}{1 + b_L a} + sa + \frac{K_c s^n a^n}{n} \quad (13)$$

where v_{H_2O} is the water concentration, a is the water activity, K_c the equilibrium constant for the clustering reaction, s the Henry's type solubility coefficient, n the mean number of water molecules per cluster, A the Langmuir capacity constant and b_L the Langmuir affinity constant. In equation (13), the first term represents the Langmuir sorption, the second one the Henry's law term and the third one is the non linear contribution of the water clusters. The parameters of the Park model have a predominant effect in a limited water activity range. Langmuir's terms, A and b_L have an influence in zone I for low water activity ($a < 0.1$). Henry's solubility coefficient, s , defines the slope of the isotherm in zone II ($0.1 < a < 0.6$). The value K_c and n could be linked to the equilibrium state corresponding to the water clusters in zone III ($a > 0.6$).

A simplified representation of the Park model has been suggested by [12] where the Langmuir sorption mechanism is not taken into account and the remaining two terms are written according to a simpler form:

$$v = Ha + ba^m \quad (14)$$

The first term is related to the linear part observed for low activities and related to the Henry's behavior. The second term is related to the non linear part that appears at high water activities, generally related to the formation of water clusters.

A possible extension of the model would be to consider a temperature dependency of Henry mechanism on temperature dependant. Equation (14) can, therefore, be modified according to:

$$v_{H_2O} = H_0 \exp\left(\frac{E_a^H}{RT}\right) \cdot a + ba^m \quad (15)$$

Figure 9 presents the comparison between the models prediction with the optimum parameters and the numerical results for the 4 tested temperatures. The best parameters are given in Table 3.

Fig. 9 – Prediction of the volume fraction of water in the amorphous phase for the modified Park model at various temperatures

Parameter	Value
H_0	0.027
E_a^H	-2642 [kJ/mol]
b	0.052
m	4.554
$DC@25^\circ C$	0.9993
$DC@40^\circ C$	0.9977
$DC@60^\circ C$	0.9954
$DC@80^\circ C$	0.9977

Tab. 3 – Optimum parameters for the modified Park model.

4.5 GAB model (1966)

The GAB model [18-20] (Guggenheim-Anderson-de Boer) is one of the most, if not the most, widely used model in the literature. The basic assumption of the model is the localization of the physical absorption in multilayers with no lateral absorption. The first sorbed molecules cover the surface and are very strongly bounded to the monolayer. Subsequently, the layers of molecules sorbed have less interaction with the sorbent surface and the range in energy levels is between those of the monolayer molecules and those of the bulk liquid. The GAB equation is expressed as:

$$v_{H_2O} = \frac{v_m K C a}{(1 - K a)(1 + K a(C - 1))} \quad (16)$$

where v_m is the monolayer value measuring the polymer availability of active sites for water molecules, a is the water activity, A is a factor correcting the properties of the multilayerer molecules relative to the bulk liquid and C is the Guggenheim constant that measures the strength of the binding of water to the primary binding sites.

The temperature dependency can be taken into account through an Arrhenius type equation, relating reaction rate constants (C_0 , K_0) with activation energies (E_a^C , E_a^K) [27].

$$C = C_0 \exp\left(-\frac{E_a^C}{RT}\right) \quad (17)$$

$$K = K_0 \exp\left(-\frac{E_a^K}{RT}\right) \quad (18)$$

where v_m is assumed as temperature independent [27], T is the absolute temperature ($^{\circ}\text{K}$) and R is the universal gas constant (8.314 J/mol/K). Figure 10 presents the comparison of the model prediction with the optimum parameters and the numerical results for the 4 tested temperatures. The best parameters are given in Table 4.

Fig. 10 – Prediction of the volume fraction of water in the amorphous phase for the GAB model at various temperatures.

Parameter	Value
v_m	0.05
K_0	0.574
E_a^K	-440 [kJ/mol]
C_0	0.563
E_a^C	-3453 [kJ/mol]
$DC@25^{\circ}\text{C}$	0.9993
$DC@40^{\circ}\text{C}$	0.9981
$DC@60^{\circ}\text{C}$	0.9948
$DC@80^{\circ}\text{C}$	0.9986

Tab. 4 – Optimum parameters for the GAB model.

6. Discussion

The complete experimental database revealed two sorption mechanisms, as classically found in the literature for PA6.6: a Henry type sorption mechanism that mainly governs the

sorption behavior at low activities and a Flory Huggins sorption mechanism at high activities. It was also noticed that the maximum water uptake is temperature dependant. The higher the temperature, the lower the maximum water uptake (for a given activity), which is a new result, contradicting some recent authors [13, 23]. This temperature dependency is attributed to the Henry contribution [12, 24, 25], *i.e.* the linear part of the curve. Our experimental observations tend to correlate the interpretation that the global shape of the curves does not change with temperature and that the linear contribution, evaluated from the initial slope, is clearly temperature dependant.

Four models were challenged to reproduce these experimental observations. In section 4.2, the Flory Huggins was identified and compared to this database. Fairly good agreement was seen for low activities, and the temperature dependency is well captured. However, a deviation between the experimental results and the model prediction appears for water activities over 0.5. Moreover, this deviation appears sooner as the temperature increases. This result can be attributed to the fact that the influence of the Henry contribution decreases as the temperature increases due to the effect of the temperature on the maximum water uptake at equilibrium. Therefore, the non linear aspect appears sooner as the temperature increased. The limitation of the Flory-Huggins model can be justified thanks to its underlying hypothesis. Indeed, the model is based on the assumption of random mixing [6] and does not take into consideration the specific interaction between the sorbent and the substrate, *i.e.* the formation of water cluster in our specific case. Therefore, the accuracy of the model is reduced for high water activities.

The ENSIC model fits better the experimental results over the whole activity range and for all the temperatures than the Flory-Huggins model. Moreover, the theoretical limitation of the Flory-Huggins model does not stand for this model since the clustering phenomenon can be taken into account. However, we can also see a slight reduction of the model accuracy at low water activity compared to the previous model, and an underestimation of the prediction at very high water activities. This specific behavior can be explained by an intrinsic limitation of the model. Indeed, the model can only describe one sorption mechanism (Langmuir, Henry, clustering) at the same time. Any combination of these phenomena is, by construction of the model, impossible. Therefore, as at least two sorption mechanisms are observed, this model is not appropriate. Besides these problems, the ENSIC model seems able to reproduce the experimental results with an acceptable precision with only 3 parameters. However, as two

different physical mechanisms are observed, the use of this model is not recommended, especially if extrapolation is needed.

The predictions are improved with the modified Park model. Within the whole water activity range and for all temperatures, the accuracy of the model is excellent, which is very interesting considering the small number of parameters (4). Moreover, every sorption mechanisms highlighted during the section dealing with experimental observations has its own mathematical functions. Therefore, this model is very appropriate for this material and extrapolation is possible as long as no additional sorption mechanism occurs.

Dealing with the GAB model, very good agreement is observed for all the temperature and all the water activities. From a visual point of view, no specific differences between the modified Park and GAB model are observable. However, this model has one additional term compared to the modified Park model and no improvement can be detected.

Some more quantitative data can be obtained while looking at Figure 11, which presents the evolution of the determination coefficient DC for all models (plotted versus their number of parameters) and for each temperature.

Fig. 11 – Comparison of the DC coefficient versus the number of parameters for the studied models.

Several points should be noted. The first is that, for each model, four data are plotted. These data corresponds to the DV value obtained for each temperature. A first comparison element between the models consists of evaluating the evolution of these values with temperature. This evolution is related to the capacity of the model to accurately predict each temperature. A small evolution with temperature means that the temperature dependency of moisture sorption is correctly taken into account, which is very important information, especially if the model predictions are extrapolated to a wider range of temperature. From Figure 11, it can be seen that the model that has the least “scattering” (evolution with temperature) is the modified Park model, suggesting that it can predict in a similar manner the experimental results for all the temperatures. On the contrary, the Flory Huggins model poorly describes the experimental data for a given temperature (here 80°C), leading to the conclusion that it cannot properly predict the temperature dependency of the sorption isotherms. We can also see that the DC

value is logically higher for more numerous. However, no differences between the Park model and the GAB model are observable, leading to the same conclusion as that given in the last paragraph. Therefore, considering the DC value and its scatter for a given model, it seems that the best model for describing the temperature dependency of water sorption in PA66 is the modified Park model.

7. Conclusions

In this study, the sorption of water in PA6.6 films and plates was studied over a wide range of temperature and water activities. The large database built revealed two sorption mechanisms. At low water activity, the water uptake at equilibrium is linearly dependent on the water activity and with an Arrhenius-like temperature dependency. Therefore, the water uptake obeys Henry's law. At high activity, a non linear contribution appears and can be related to the creation of water clusters. These experimental observations were compared to classical physically-based sorption models. It was found that the Flory Huggins is not able to reproduce the experimental data at high water activities. The predictions are far better using the ENSIC model, but a limitation on the number of sorption mechanism prevents the recommendation of this model for PA66. GAB and modified Park models are equivalent (from a predictability point of view) since they are able to reproduce the experimental data for every temperature and the full range of water activities. However, the modified Park model has a simpler mathematical formulation directly related to the sorption mechanism, and has one parameter less compared to the GAB model. This model is, therefore, recommended to predict the temperature dependency of the maximum water sorption in PA66.

References

- [1] A. Launay, Y. Marco, M.H. Maitournam and I. Raoult, Modelling the influence of temperature and relative humidity on the time-dependant mechanical behavior of a shortglass fiber reinforced polyamide, *Mechanics of Materials*, 56:1-10:2013.
- [2] H.K. Reimschuessel, Relationships on the effect of water on glass transition temperature and Young's modulus on nylon 6, *Journal of Polymer Science: Polymer Chemistry Edition*, 16:1229–1236, 1978.
- [3] P.E. Bretz, R.W. Hertzberg and J.A. Manson, Influence of absorbed moisture on fatigue crack propagation behaviour in polyamides, *Journal of Materials Science*, 16:2061-2069, 1981.
- [4] D. Valentin, F. Paray and B. Guetta, The hygrothermal behaviour of glass fibre reinforced Pa66 composites: A study of the effect of water absorption on their mechanical properties, *Journal of Materials Science*, 22:46-56, 1987.
- [5] R. Puffr and J. Sebenda, On the structure and properties of polyamide. XXVII. The mechanism of water sorption in polyamides, *Journal of Polymer Science Part C: Polymer Symposia*, 16:79-93, 1967.
- [6] L.-T. Lim, I.-J. Britt, and M.-A. Tung, Sorption and transport of water vapor in nylon 6,6 film, *Journal of Applied Polymer Science*, 71:197–206, 1999.
- [7] M. Akay, Moisture absorption and its influence on the tensile properties of glass-fibre reinforced polyamide 6.6, *Polymers & polymer composites*, 2:349–354, 1994.
- [8] L. Monson, M. Braunwarth, and C. W. Extrand, Moisture absorption by various polyamides and their associated dimensional changes, *Journal of Applied Polymer Science*, 107:355–363, 2008.
- [9] J.A. Barrie and D. Machin, Sorption effects in the measurement of the time lag for water vapor, *Journal of Applied Polymer Science*, 12:2633–2638, 1968.
- [10] S. Brunauer, *The Adsorption Of Gases And Vapors Vol I*. Oxford University Press, 1943.
- [11] P.-Y. Le Gac, G. Roux, P. Davies, B. Fayolle and J. Verdu. Water clustering in polychloroprene. *Polymer*, 55(12):2861-2866, 2014.
- [12] E. Gaudichet-Maurin, F. ThomINETTE, and J. Verdu, Water sorption characteristics in moderately hydrophilic polymers, Part 1: Effect of polar groups concentration and temperature in water sorption in aromatic polysulfones, *Journal of Applied Polymer Science*, 109:3279–3285, 2008.
- [13] C. El Mazry. Durabilité de produits innovants de robinetterie en polyamide 6.6. Phd Thesis ENSAM Paris, 2013.

- [14] P. Flory, Thermodynamics of high-polymer solutions. *Journal of Chemical Physics*, 10:51-61, 1942.
- [15] M. Huggins, Thermodynamics properties of solutions of long-chain compounds, *Annals of the New York Academy of Science*, 43:1-32, 1942.
- [16] E. Favre, Q.T. Nguyen, R. Clément and J. Néel, The engaged species induced clustering (ENSIC) model: a unified mechanistic approach of sorption phenomena in polymers, *Journal of Membrane Science*, 117,227:236, 1996.
- [17] G.S. Park, Transport principles – solution, diffusion and permeation in polymer membranes, *Synthetic Membranes: Science, Engineering and Applications*, 181:57-107, 1986.
- [18] E.A. Guggenheim, Application of statistical mechanics, Oxford: Clarendon Press, 1966.
- [19] R.B. Anderson, Modification of the Brunauer, Emmet and Teller equation. *Journal of the American Chemical Society*, 68:686-691, 1946.
- [20] J.H. de Boer, The dynamic character of adsorption, Oxford: Clarendon Press, 1953.
- [21] G. W.Ehrenstein, R.P. Theriault. Polymeric materials: structure, properties, applications. *Hanser Verlag*. pp. 67–78, 2001.
- [22] H. Feng, Modeling of vapor sorption in lglassy polymers using a new dual mode sorption model based on multilayer sorption theory, *Polymer*, 48:2988-3002, 2007.
- [23] B. Ledieu, Vieillissement en milieu eau/glycol du polyamide 66 renforcés de fibres de verre courtes pou l'application boîte à eau de radiateur de refroidissement moteur, *Thèse de doctorat*, ENSAM Bordeaux, 2010.
- [24] A. Tcharkhtchi, P. Y. Bronnec, and J. Verdu, Water absorption characteristics of diglycidylether of butane diol–3,5-diethyl-2,4-diaminotoluene networks, *Polymer*, 41:5777–5785, 2000.
- [25] I. Merdas, F. ThomINETTE, A. Tcharkhtchi, and J. Verdu, Factors governing water absorption by composite matrices, *Composites Science and Technology* , 62:487–492, 2002.
- [26] E. Jones, T. Oliphant, and P. Peterson, “SciPy: Open source scientific tools for Python,” <http://www.scipy.org>, 2001.
- [27] Z. B. Maroulis, E. Tsami, D. Marinos-Kouris, and G. D. Saravacos, Application of the GAB model to the moisture sorption isotherms for dried fruits, *Journal of Food Engineering*, 7:63–78, 1988.

List of figures

Fig. 1 – TrelleborgVibracoustic engine mount with PA6.6 50% wtGF housing for PSA.

Fig. 2 – Example of DVS result obtained for a temperature of 40°C. The mass evolution $\Delta m = m_t - m_0$ is plotted versus time.

Fig. 3 – Comparison between DVS measurements and classical gravimetric analysis for a temperature of 25°C.

Fig. 4 – Sorption curves for all the testing temperature.

Fig. 5– Effect of the temperature on the sorption curves.

Fig. 6 – Effect of the temperature on the nonlinear contribution of the sorption curves obtained by subtracting the linear contribution evaluated experimental data for water activities up to 0.4

Fig. 7 – Prediction of the volume fraction of water in the amorphous phase for the Flory-Huggins model at various temperatures.

Fig. 8 – Prediction of the volume fraction of water in the amorphous phase for the ENSIC model at various temperatures.

Fig. 9 – Prediction of the volume fraction of water in the amorphous phase for the modified Park model at various temperatures.

Fig. 10 – Prediction of the volume fraction of water in the amorphous phase for the GAB model at various temperatures.

Fig. 11 – Comparison of the DC coefficient versus the number of parameters for the studied models.

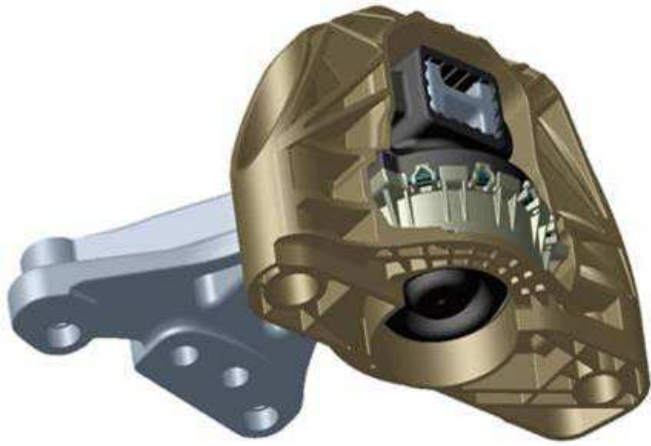
List of tables

Tab. 1 – Optimum parameters of the Flory Huggins model

Tab. 2 – Optimum parameters of the ENSIC model

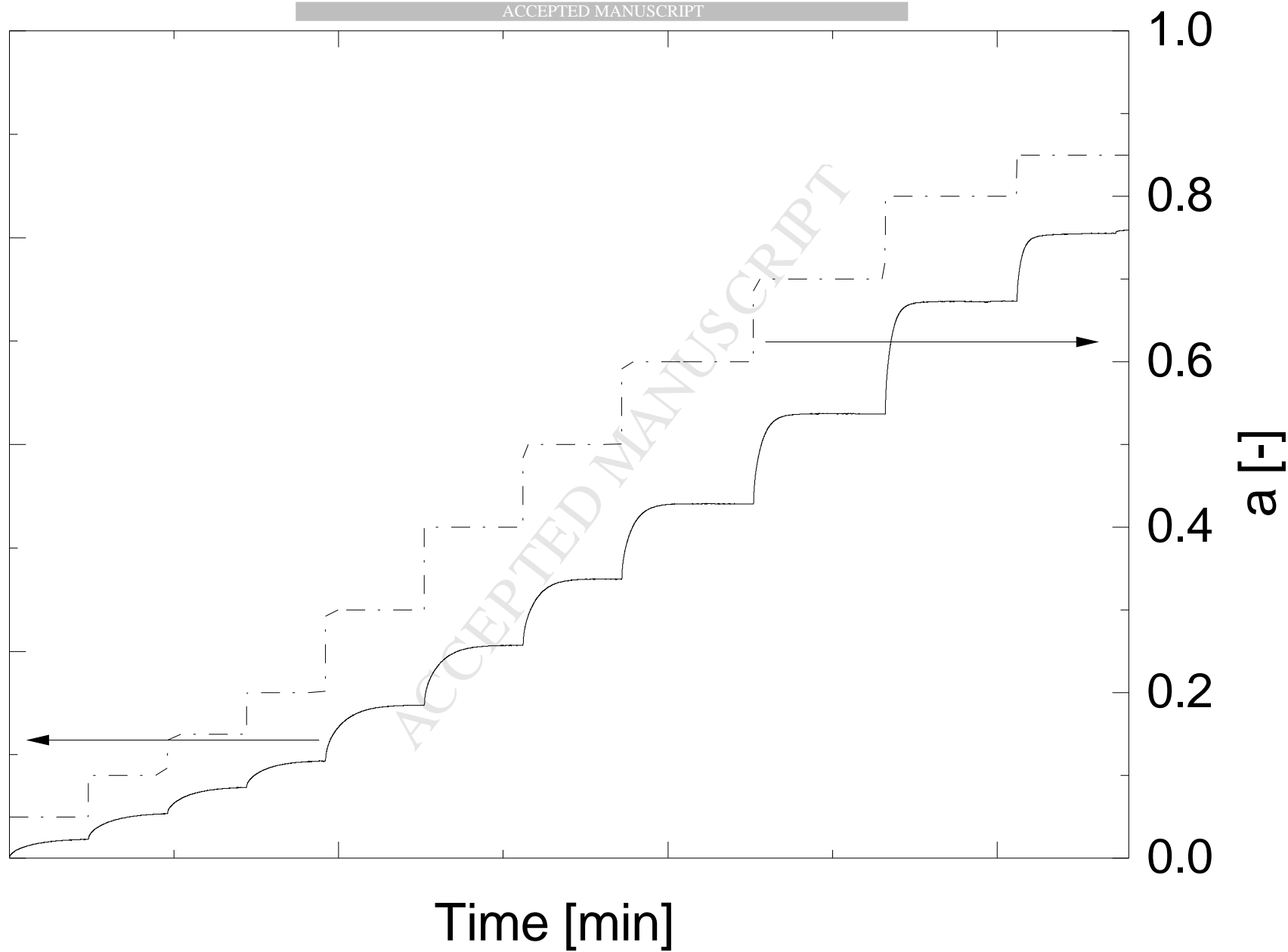
Tab. 3 – Optimum parameters of the modified Park model

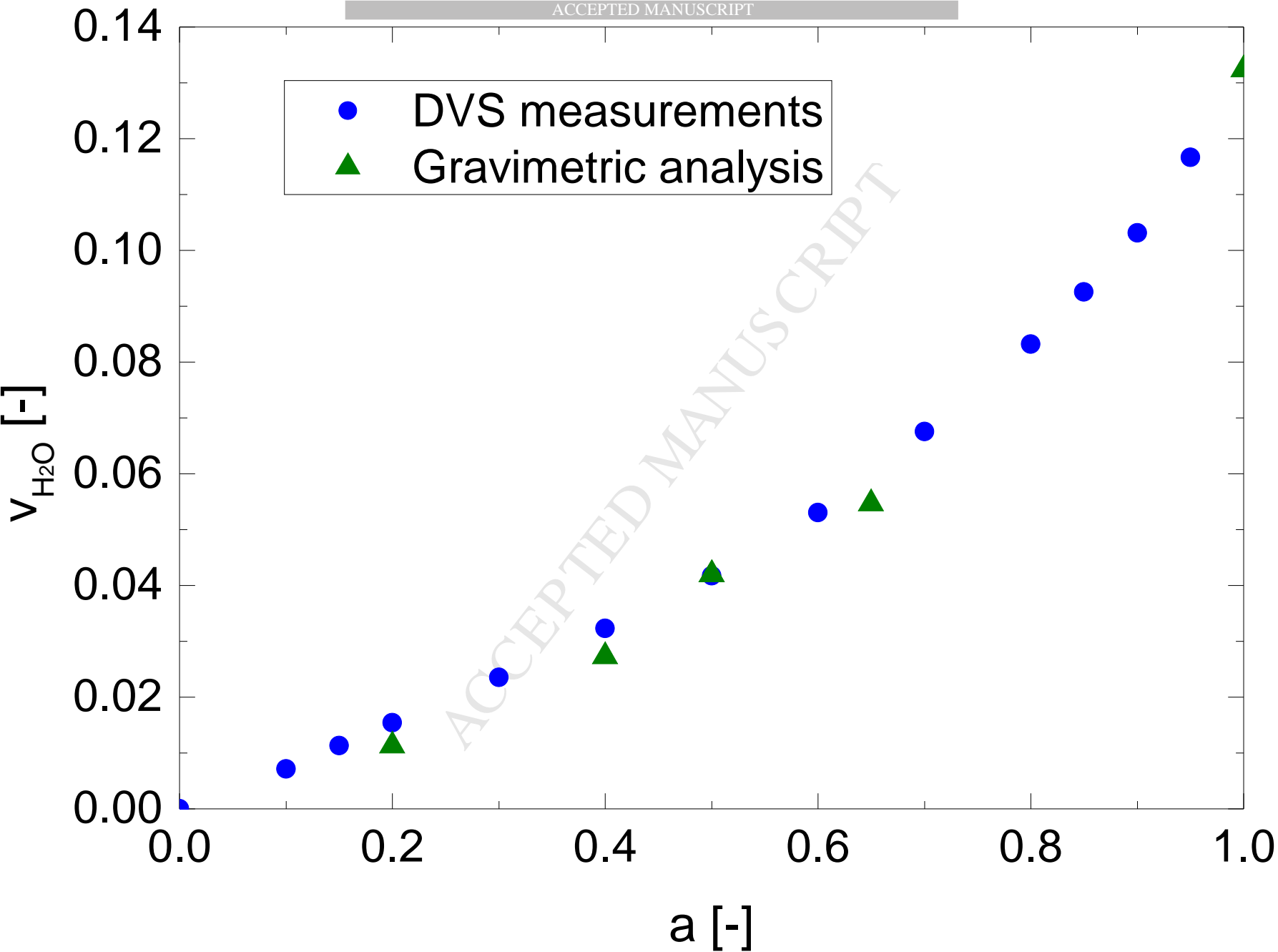
Tab. 4 – Optimum parameters of the GAB model

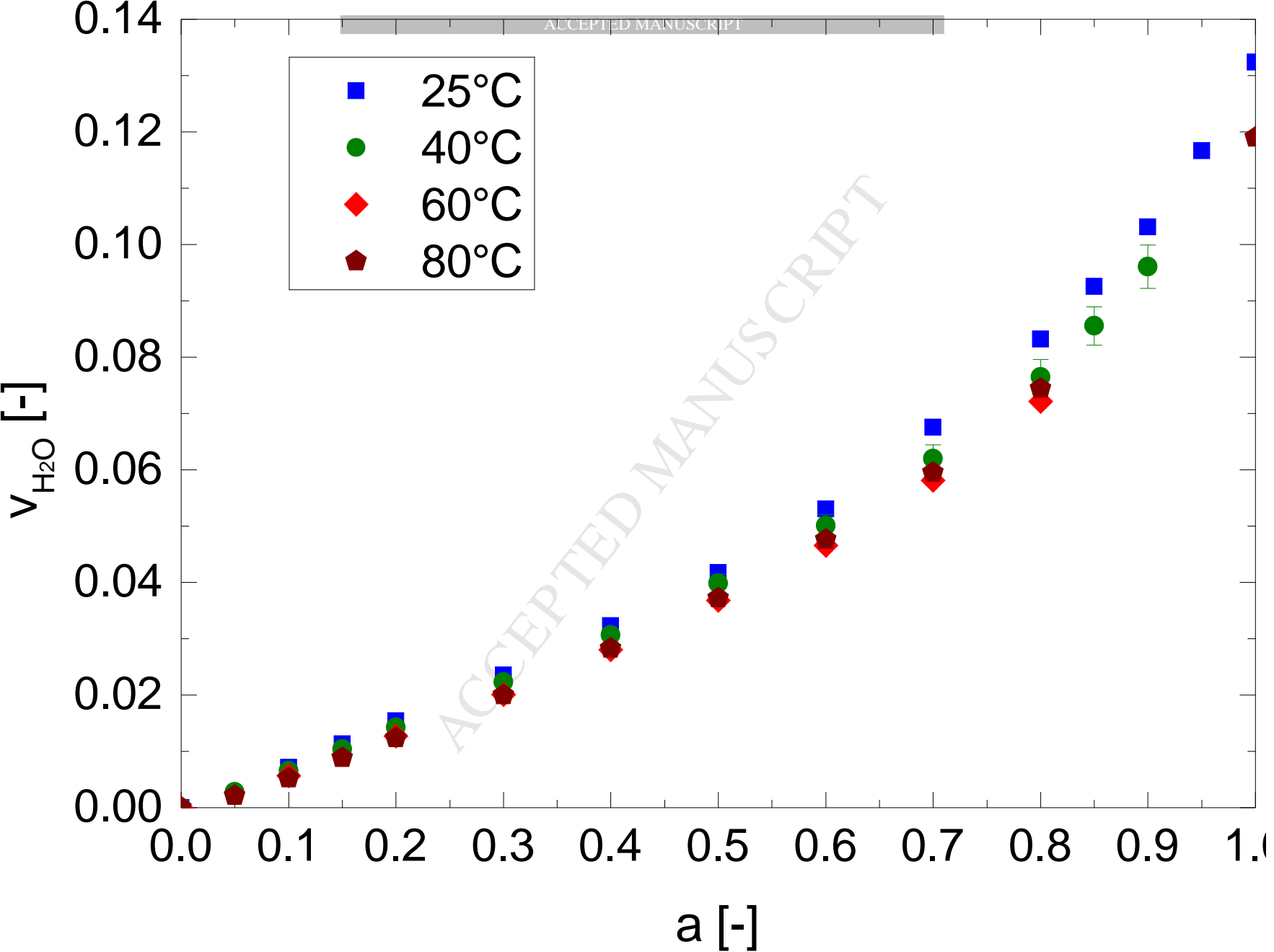


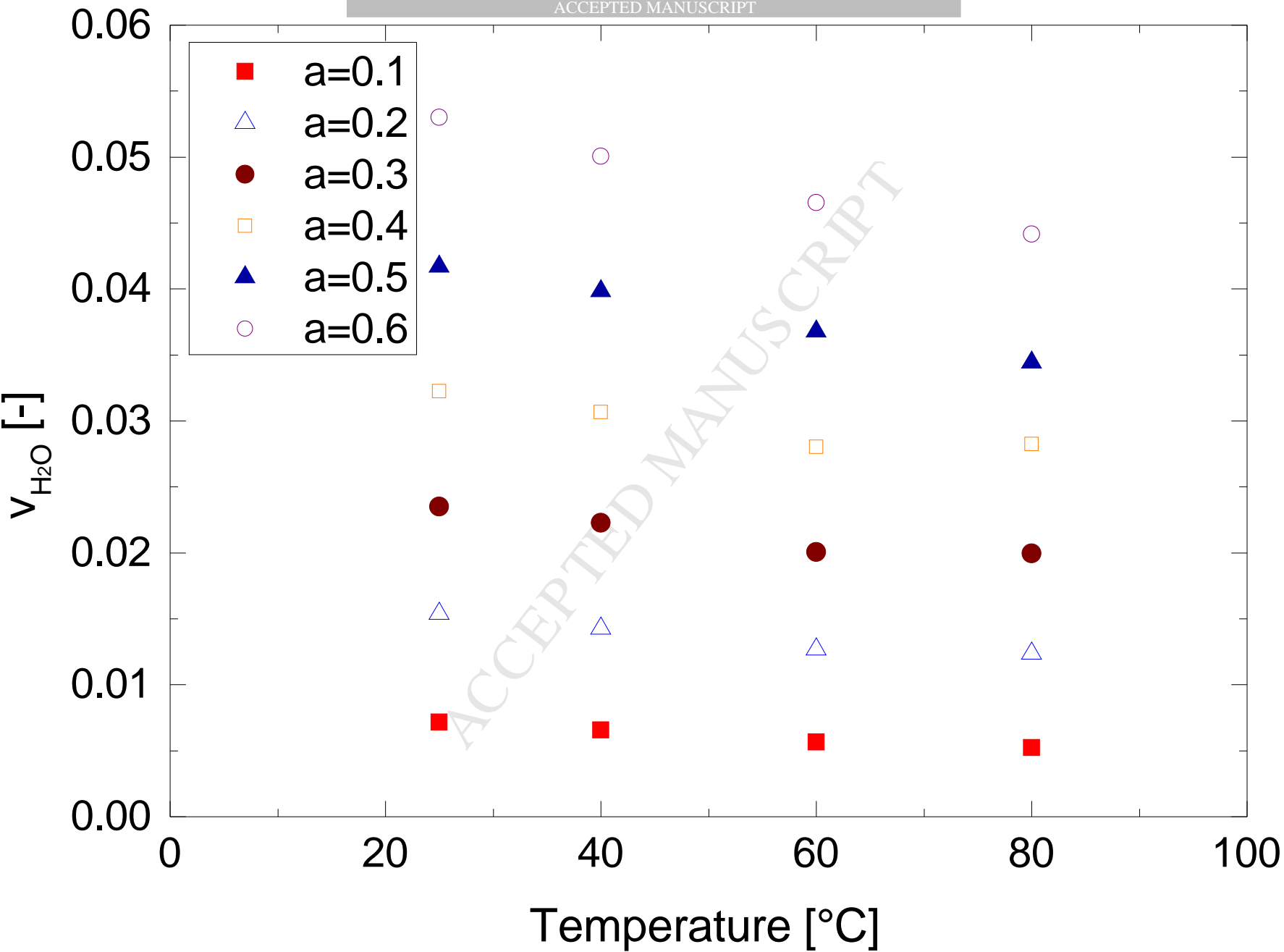
ACCEPTED MANUSCRIPT

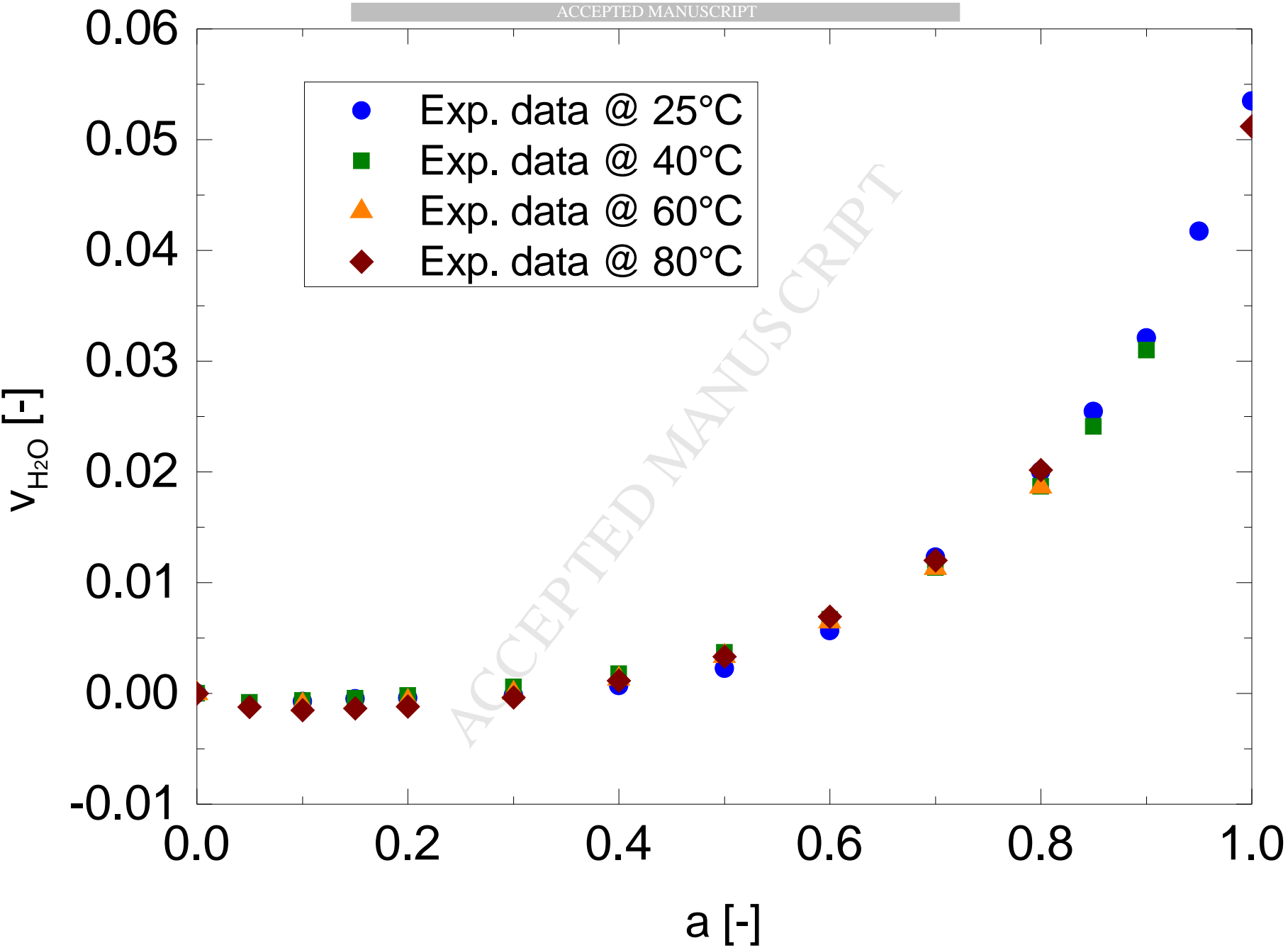
Mass evolution [mg]

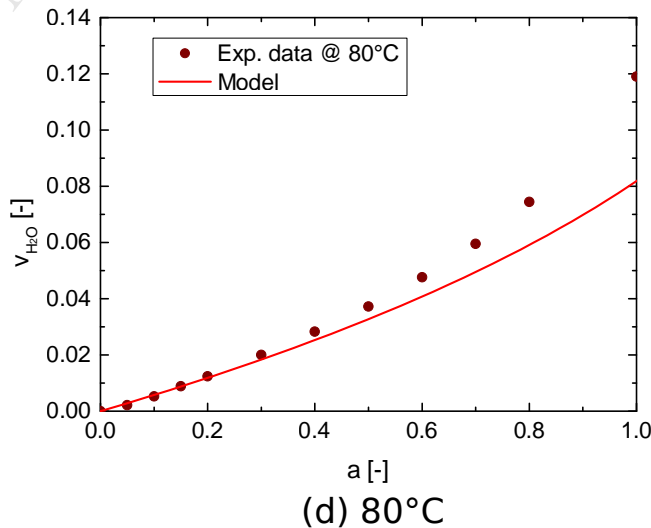
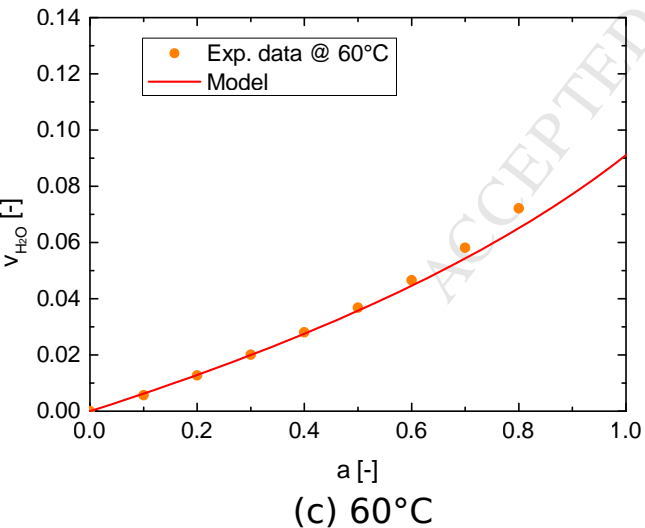
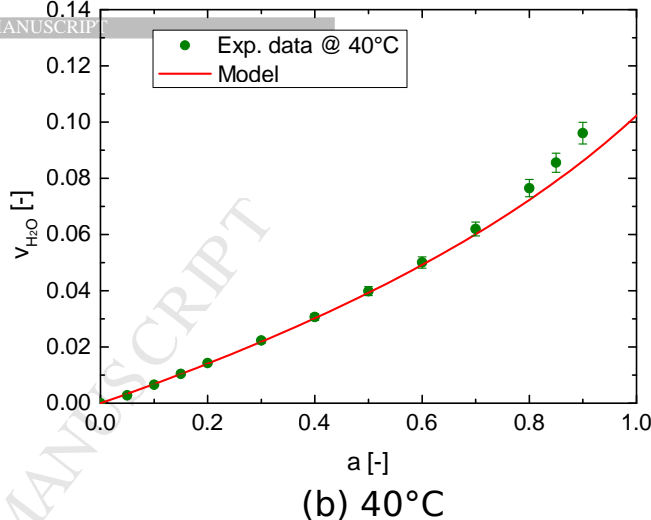
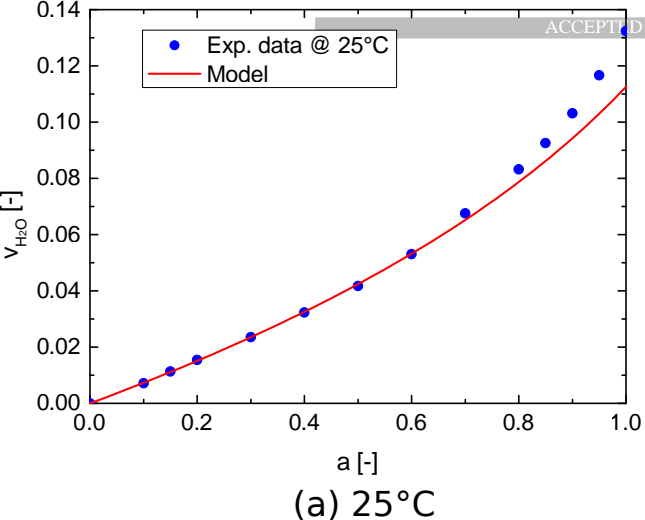


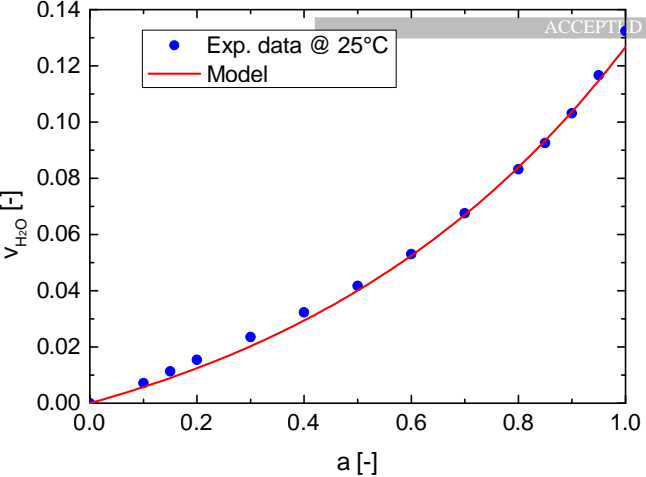




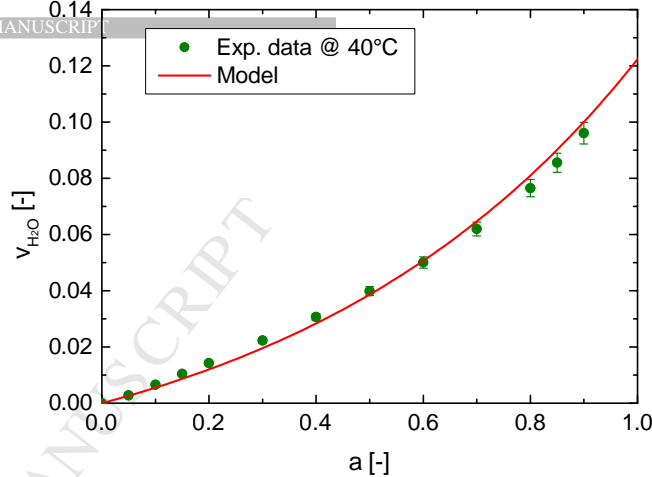




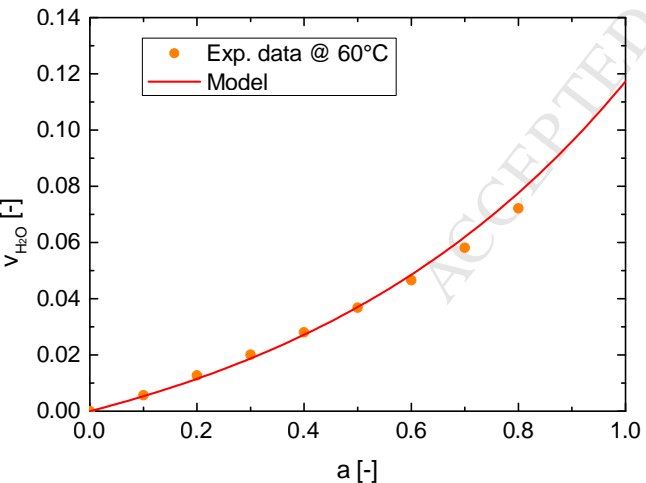




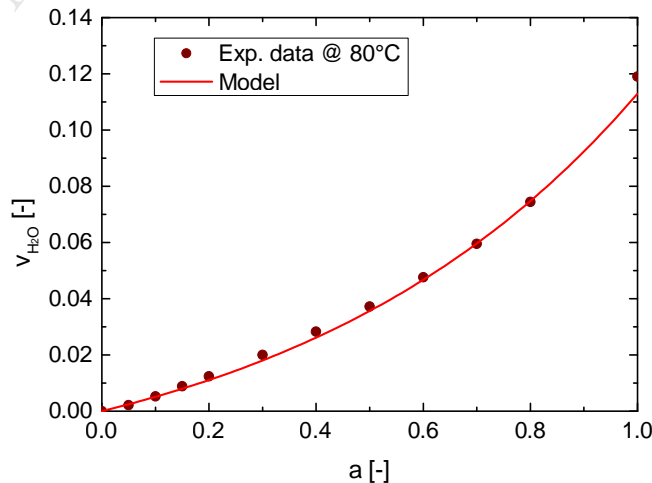
(a) 25°C



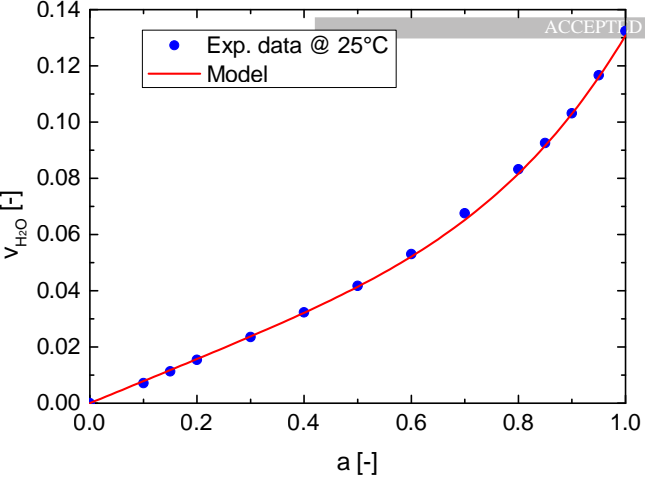
(b) 40°C



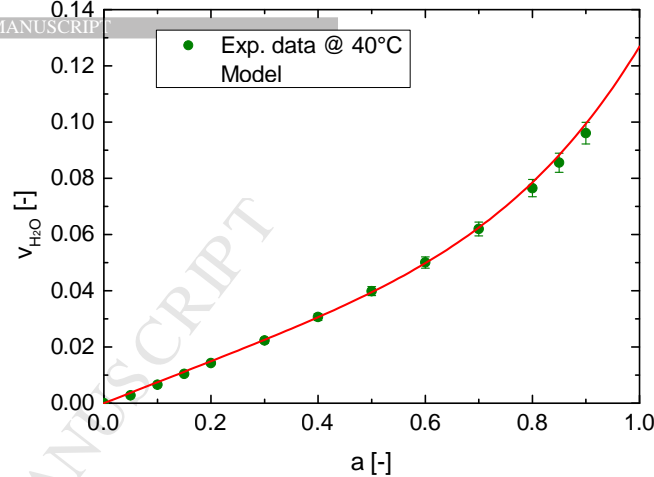
(c) 60°C



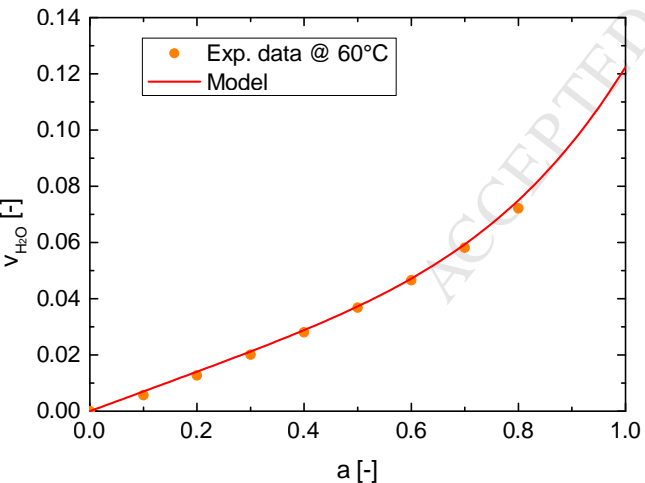
(d) 80°C



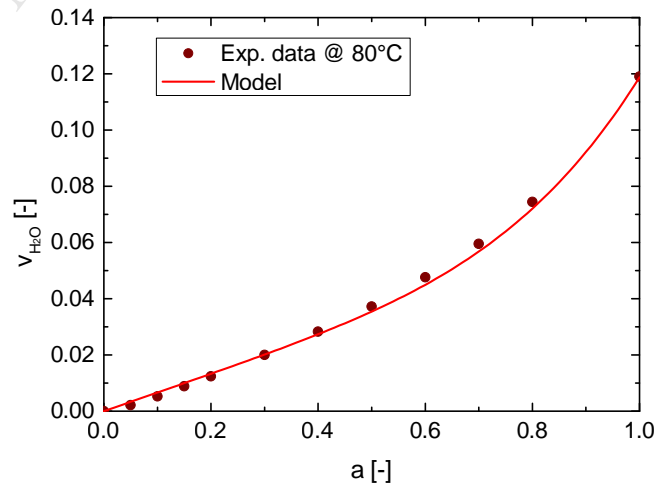
(a) 25°C



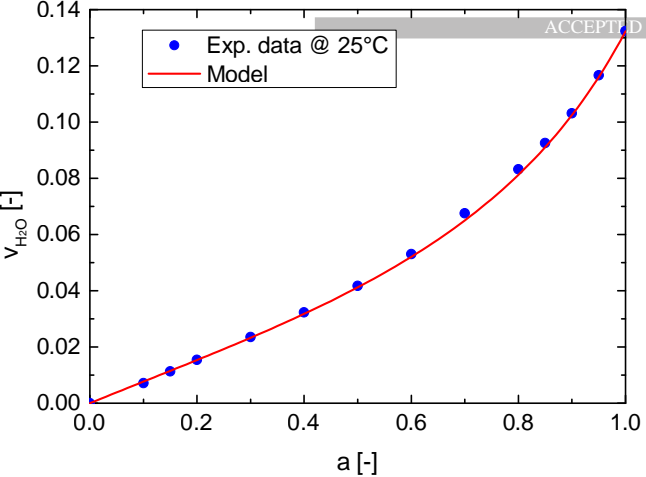
(b) 40°C



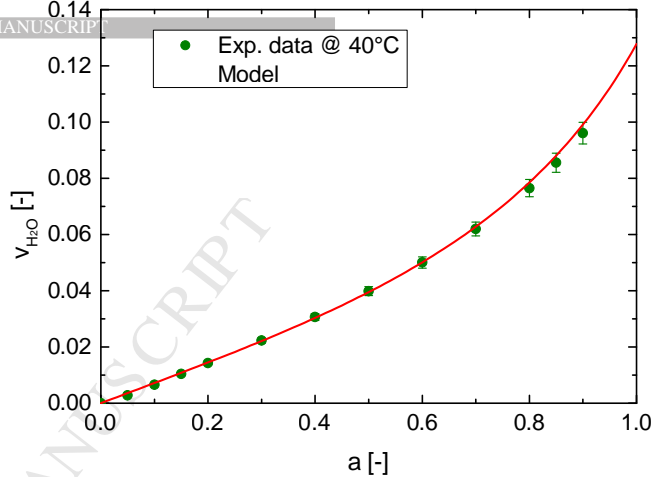
(c) 60°C



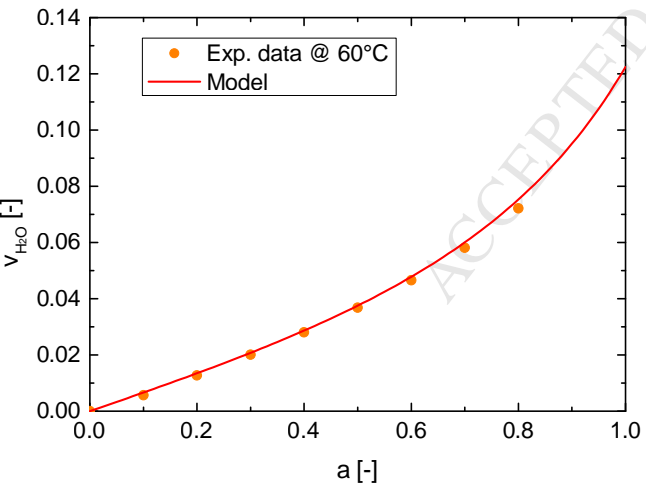
(d) 80°C



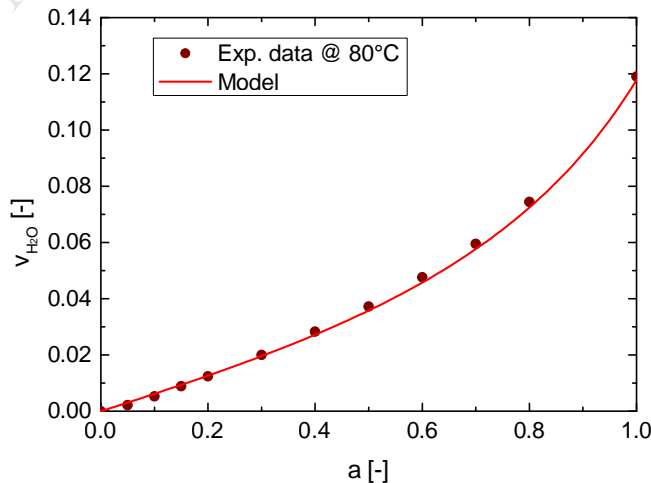
(a) 25°C



(b) 40°C



(c) 60°C



(d) 80°C

